11th International Conference on Fracture Mechanics of Concrete and Concrete Structures
FraMCoS-11
J. M. Chandra Kishen, A. Ramaswamy, S. Ray and R. Vidyasagar (Eds)
https://doi.org/10.21012/FC11.092336

STUDY ON INTERFACE FRACTURE AND FAILURE MODES IN STEEL PLATE AND CONCRETE EMBEDMENT

A SELVA GANESA MOORTHI [*], G APPA RAO[†]

[*] Department of Civil Engineering, IIT Madras, Chennai, India.
e-mail: selvaganeshgce@gmail.com

[†] Department of Civil Engineering, IIT Madras, Chennai, India.
e-mail: garao@iitm.ac.in

Key words: Bond, Pull-out test, Embedment length, Bond-slip model, Interface

Abstract: Interface between connecting steel plates and concrete plays an important role on performance of precast reinforced concrete shear wall system. Embedded steel plate provides dry connection with prefabricated panels as bolted or welded plate connection via anchoring rods or bolts during fabrication process. Recently, prefabricated techniques gained momentum due to time and material savings, enhanced quality control and increased efficiency with sustainability. Connection in precast system alters failure mode of the entire system by improving damage resistance. This paper describes the pull-out bond tests performed on a steel plate embedded in concrete using three distinct methods of anchoring to analyze behavior of steel plate-concrete embedment under tension loading. The test specimen consists of steel plates embedded in concrete blocks with three different anchoring schemes by a) rod, b) bolt and c) bolt with washer nut arrangement as anchorage and different number of bolts. The steel plates were connected to a loading frame through bolts and nut system, and then transferred the load to the plate to measure the slip with reference to concrete surface. The load-displacement response of the connection has been monitored, and the failure modes were examined. The test results have been compared with the existing analytical model to determine the pull-out bond behaviour and influence of number of bolts and the concrete strength. Anchoring using bolt and washer nut system performed better than the other anchoring methods.

1 INTRODUCTION

Precast system offers several advantages for a better choice in the construction industry. One key benefit is the faster construction timeline. Since precast components are manufactured in off-site under a controlled environment, the process of assembling them on-site is possible in shorter durations. Additionally, the quality of precast components is closely monitored and maintained, leading to consistent and high-quality construction. Cost-effectiveness is another advantage [1,2,3]. An efficient manufacturing process reduces labour and maintenance costs, making it a more economical option relative to traditional construction methods. Moreover, precast construction offers design flexibility, allowing for customization and architectural versatility. Various shapes, sizes, and finishes can be achieved to satisfy specific project requirements. Precast construction is a sustainable building method [4] that reduces construction waste [5], improves energy efficiency, promotes durability, and incorporates recycled materials. It also offers efficient site management, supports reusability and recyclability, and contributes to water conservation. Overall, it is an environmentally friendly choice for sustainable practices.

Embedded plates play a critical role in precast connections [6,7,8] serving as essential

means for load transfer and ensuring structural integrity of the overall system. These plates are designed to efficiently distribute forces such as shear, moment, and axial loads between precast elements, enabling them to work together as a unified structure. By enhancing joint strength, embedded plates provide robust connections that can withstand external forces and maintain stability. These plates also contribute to connection rigidity, minimizing movement and displacement between precast elements and reducing the risk of deformations or cracks. The embedded plates offer design flexibility, allowing for various connection configurations to suit project-specific requirements. Their presence simplifies installation by providing pre-designed connection points, ensuring accurate positioning and alignment during assembly. Moreover, embedded plates are designed to be durable, corrosion-resistant, and capable of withstanding long-term use, thus ensuring longevity and performance of connection. Ultimately, embedded plates play a vital role in enhancing performance of precast systems, optimizing load distribution, and ensuring overall safety and integrity of the structure.

The pull-out test is widely used for assessing the bond strength between embedded plates and concrete in precast construction. This test involves subjecting a concrete specimen containing an embedded plate to a gradually increasing tensile force until failure occurs. The test set-up includes instrumentation such as load cells or hydraulic jacks to apply and measure the force. As the force increases, failure of the bond between the embedded plate and concrete takes place, which can manifest in different modes such as plate detachment or concrete cone failure.

This study investigates the plate embedment in concrete using different methods, including plain rod, threaded rod, stud, and bolt with washer nut arrangement. Specifically, the bolt with washer nut arrangement is further examined by considering two numbers and embedment in the grout. The experimental results obtained from the lab test are validated by utilizing an analytical bond slip curve, which is based on the interface fracture energy.

2 THEORETICAL BACKGROUND

Threaded anchors can be broadly categorized into three main types based on their anchoring mechanisms: mechanical interlock, friction, and bond. These mechanisms play a crucial role in transferring loads to the surrounding construction [9,10,11,12,13]. In the case of mechanical interlock, the connection between the bolt head element and the adjacent concrete establishes a strong interlocking mechanism. This allows shear forces to be effectively transmitted through the anchor's surface and its specific shape [14]. On the other hand, bond relies on the expansion forces generated by the anchor and the resulting frictional forces. When a fully threaded bolt expands, it significantly increases the frictional force, thereby enhancing the anchor's resistance against pull-out. Understanding and analyzing these anchoring mechanisms provides valuable insights into the behavior and performance of threaded anchors in various construction scenarios.

2.1 Failure mode

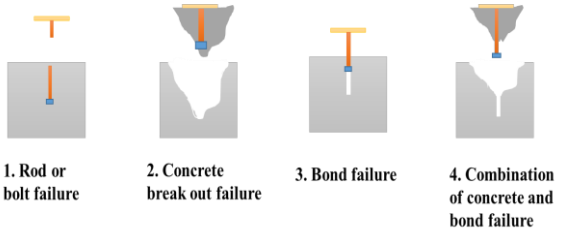

Figure 1: Failure modes in pull-out loading

Depending on the overall geometry and embedment length, there are four possible modes of failure [15] as shown in the Figure 1. Rod failure is defined as the occurrence when the applied load exceeds the tensile strength of the steel during testing. This situation typically arises when anchors are having relatively more embedment lengths. Concrete blowout happens when the tensile strength of the concrete is surpassed, and there hasn't been any other failure mode prior to it. In this case, a cone-shaped fragment of concrete (with an angle of approximately 35°) typically breaks out along with the anchors [16,17,18, 19]. If the

bond stress between steel and concrete is low due to factors such as cracked concrete or low concrete strength, it can lead to steel/concrete bond failure and the extraction of the rod. In models that describe the resistance at the bonded interface, it is assumed that the failure surface occurs adjacent to the surface of the embedded portion of the anchor at the anchor-to-concrete interface. The critical parameter in these models is the bond stress at the anchor-to-concrete interface, which is typically assumed to be uniformly distributed over the area of the failure surface. The final one is combination of both bond failure and concrete cone break out.

3 EXPERIMENTAL PROGRAMME

3.1 Test matrix

The experimental study involved testing of different specimens, categorized by the codes in Table 1: SP (specimen), P (plain rod), T (High Yield Strength Deformed (HYSD) bar), S (stud - fully threaded 4.6 grade M_{12} bolt), B (fully threaded 4.6 grade M_{12} bolt with washer nut arrangement), and G (grout). Each category comprises two specimens, which were cast, tested, and their average values are reported. Standard cube specimens measuring 150 mm x 150 mm x 150 mm were used for testing. Prior to casting, a 20 mm diameter pull-out rod (made of Fe550 D steel) was welded onto one face of the plate (50 mm x 50 mm x 10 mm) intended for embedding in concrete. Different types of anchoring rods or bolts were welded onto another face to facilitate testing. Except for the SP6 G specimens, concrete with compressive strength of 36 N/mm² is used and for SP6 G specimen Fosroc conbextra grout having compressive strength of 73 N/mm² is used.

For SP1 P, SP2 T, and SP3 S specimens, an embedment length of 60 mm was achieved by directly welding rods or studs onto a 50 mm x 50 mm x 10 mm plate. In the case of SP4 B, SP5 B2, and SP6 G categories, a hole was drilled in the plate, tapped to create threads, and then a bolt was inserted into the hole and welded. Therefore, the effective embedment length for these categories was 50 mm, shown in Figure 2.

Table 1: Test Matrix

Specimen code	f_{ck} for concrete in N/mm²	Embedment length in mm
SP1 P	36	60
SP2 T	36	60
SP3 S	36	60
SP4 B	36	50
SP5 B2	36	50
SP6 G	73	50

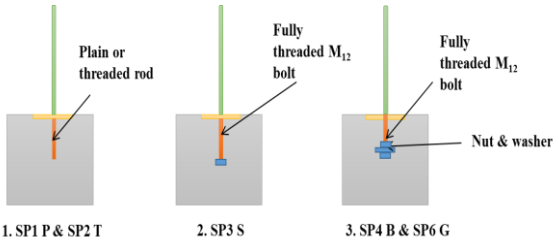

Figure 2: Specimen details for pull - out test

3.2 Experimental Set-up

The pull-out test set-up shown in Figure 3 comprises various components that enable accurate load application and displacement measurement. A concrete specimen with standardized dimensions is prepared, and the anchor, such as a rod, stud, or bolt, was embedded into it at a specified embedment length. To apply the load a universal testing machine was used. This equipment exerts an axial load on the extended 20 mm diameter bar at the end of the anchor. The applied load during the test is accurately measured. To ensure stability and prevent undesired movement or rotation, a reaction system is utilized. It provides support to the concrete specimen, allowing the load to be solely applied to the anchor without any disturbances. The load is then gradually increased in a controlled manner. Throughout the test, the applied load is continuously slip is measured using Linear Varying Differential Transformer (LVDT). The test continues until the anchor begins to pull out from the concrete or until the desired failure mode is observed. The failure mode, such as bond failure or concrete blowout, is carefully observed and recorded for further analysis.

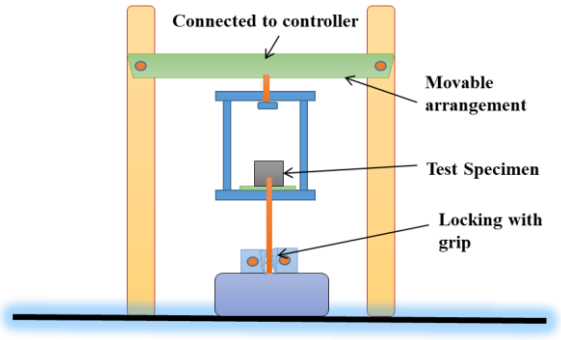

Figure 3: Experimental set-up

All specimens underwent a load-controlled pullout test, where the load (kgs) and slip (mm) were measured. However, the observed post-peak behavior has certain limitations due to the load control system employed, and the failure mode was observed as shown in Figure 4.

Figure 4: Pull-out test in laboratory

4 EXPERIMENTAL RESULTS

4.1 Test results

The experimental study conducted on various specimens, with the peak load and failure modes documented in Table 2. Except for specimens SP1 P and SP4 B, all the specimens experienced concrete breakout failure. Specimen SP1 P, which comprised a plain rod, failed due to bonding failure. This occurred because there is no ribbing for improved bonding, resulting in sudden failure. Specimen SP4 B exhibited a failure mode characterized by a combination of concrete break out and yielding of the washer due to its lesser thickness.

Table 2: Peak load and failure mode

Specimen code	Peak load in kg	Failure mode
SP1 P	800.5	Bond failure
SP2 T	2439	Concrete breakout
SP3 S	2599.3	Concrete breakout
SP4 B	2712.3	Concrete breakout + washer yield
SP5 B2	4062.2	Concrete breakout
SP6 G	2999.5	Concrete breakout

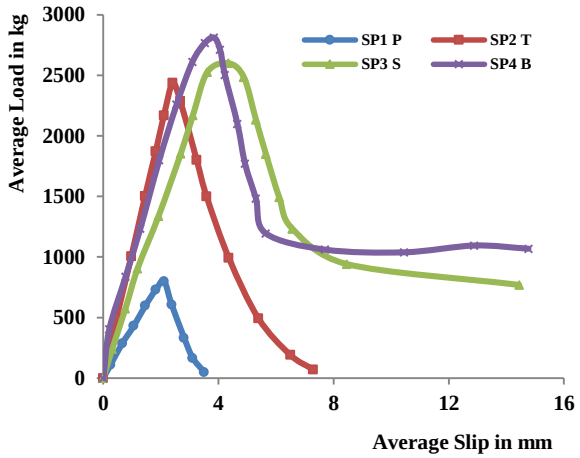

Figure 5: Peak load vs. slip (SP1 P, SP2 T, SP3 S & SP4 B)

SP4 B exhibits a higher peak load compared to all other specimens with the same concrete. SP3 S also demonstrates a similar peak load, albeit with a slightly greater embedment length than that of SP4 B. SP1 P fails due to bond and displays a brittle behavior at a very low load. SP2 T used high yield strength deformed rods, to withstand a sufficient peak load but experiences sudden brittle failure afterward. Figure 5 clearly indicates that SP4 B achieves a higher peak load despite a shorter embedment length and demonstrates superior post-peak behavior, as the diameter of the washer is greater than that of the bolt head. Hence very good interlocking.

Increasing the number of embedded bolts improves both the peak load and post-peak behavior. Introducing two bolts in SP5 B2

resulted in a 50% increase in the load. Another method to enhance the peak load is by increasing the strength of the concrete. In the case of SP6 G, peak load increased by 10.6%. However, it is important to note that grout lacks significant post-peak behavior and instead exhibits sudden brittle failure as shown in Figure 7. In the grout there is no coarse aggregate hence brittle failure is taking place. Figure 6 clearly indicates that SP4 B, SP5 B2 and SP6 G achieve a peak load at same slip level of 4.5 to 4.8 mm.

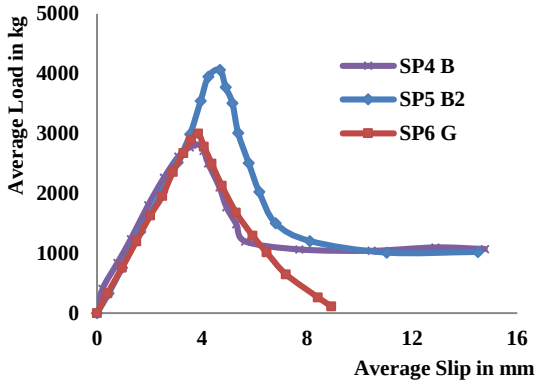

Figure 6: Peak load and slip-SP4 B, SP5 B2 and SP6 G

Figure 7: Typical concrete cone break out (SP6 G)

5 ANALYTICAL MODEL

5.1 Bond slip model

The pullout response in all specimens is predicted by employing the bond-slip model, derived from the analysis, which is specifically designed to analyze the carbon fiber-reinforced polymer (CFRP)-to-concrete interface [20]. This model incorporates the concept of interface fracture energy (G_f) as a fundamental parameter for accurate estimation.

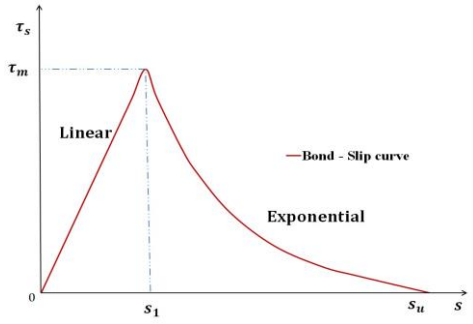

Figure 8: Bond - slip model for pull - out

The bond-slip curves depict three distinct stages: the initial linear stage, subsequent nonlinear stage, and final constant stage [21,22,23]. These stages can be represented by a linear equation for the ascending portion and an exponential form for the descending branch. It also demonstrates that the local bond-slip curves can be divided into three parts, which align with the three stages in the strain-slip curves. By considering the shape of the bond-slip curve in Figure 8, it is possible to express the shear stress in the following [20,24,25].

$$\tau(s) = \begin{cases} \tau_m \left(\frac{s}{s_1}\right) & s \le s_1 \\ \tau_m \, e^{-\omega(s-s_1)} & s_1 \le s \le s_u \\ 0 & s_u \le s \end{cases} \quad (1)$$

The shear stress, τ(s), corresponds to the stress experienced at a given bond slip value (s), with τ_m representing the Peak shear stress, and s_1 representing the slip corresponding to peak shear stress. The Interfacial Fracture Energy (G_f) is defined as the enclosed area under the bond-slip curve for the interface between the anchoring rods or bolts and concrete. To calculate the interfacial fracture energy, the following equations (2) and (3) can be used:

$$G_f = \int_0^\infty \tau \, ds = \int_0^{s_1} \tau \, ds + \int_{s_1}^\infty \tau \, ds \quad (2)$$

$$G_f = \frac{1}{2} \tau_m \, s_1 + \int_{s_1}^\infty \tau_m \, e^{-\omega(s-s_1)} \, ds \quad (3)$$

$$\int_{s_1}^\infty \tau_m \, e^{-\omega(s-s_1)} \, ds = \frac{\tau_m}{\omega}$$

The coefficient ω can be expressed as in Eq. (4), which is derived from the equation (3),

$$\omega = \frac{\tau_m}{G_F - \frac{1}{2}\tau_m \, s_1} \quad (4)$$

The bond-slip model can be described using

several important parameters such as, τ_m s_1, s_u, and ω. Notably, these parameters can be determined based on the interfacial fracture energy (G_f). Once these key parameters are established, it becomes possible to derive the bond-slip behaviour of pull-out test.

5.2 Peak bond stress

Peak bond stress is determined by dividing the peak load with the interface area based on observed experimental results. Figure 9 clearly shows that specimens with M_{12} bolts achieve peak bond stress within the slip range of 3.8 to 4.8 mm, primarily due to the bearing action of the head. When calculating bond shear stress, the head diameter is taken into account. On the other hand, plain or threaded rods reach peak bond stress in the slip range of 2 to 2.5 mm. The strength of the concrete plays a significant role in determining peak bond stress, so that the grout specimen exhibits higher bond stress failure, resulting in concrete breakout. For the plain rod, both bond stress and slip are very low because of slipping mode of failure.

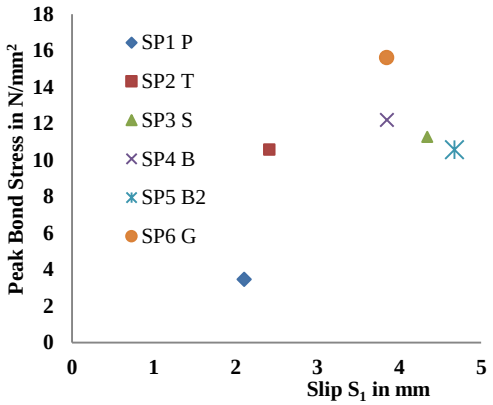

Figure 9: Peak bond stress with slip s_1

5.3 Interface fracture energy

Interface fracture energy (G_f) is the measure of the energy required to cause bond failure, calculated as the area under the bond load-slip curve. In Figure 10, G_f is determined for all specimens in both the elastic and plastic ranges. SP5 B2 has a larger interface area, resulting in higher interface fracture energy. Conversely, SP6 G has a lower interface fracture energy compared to SP4 B. Increasing the strength of the concrete can enhance peak bond stress and elastic energy, but it leads to a decrease in the total interface fracture energy, making the failure more brittle. Consequently, SP4 B outperforms the others due to its smaller interface area

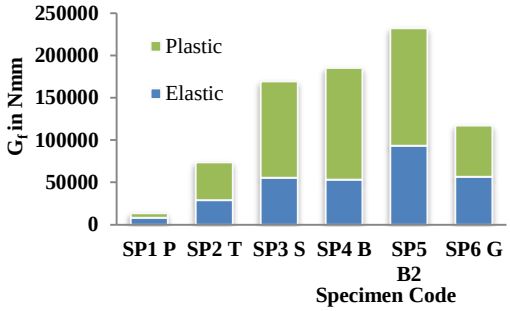

Figure 10: Interface fracture energy G_f

5.4 Coefficient ω

The coefficient ω in the context of the pull-out test serves as a quantitative measure of the rate at which the post-peak response decays. A higher value of the coefficient ω indicates a rapid exponential decline in the post-peak curve, which is characteristic of a more brittle behavior. On the other hand, a lower value of the coefficient ω signifies a slower decay in the post-peak curve, suggesting a less brittle response. Therefore, the coefficient ω provides valuable information about the brittleness of the material or system under consideration in the pull-out test. SP1 P (plain rod) is having higher coefficient and exhibited brittle failure. SP4 B (Bolt with washer nut arrangement) is having lower; it performed well than others as shown in Figure 11.

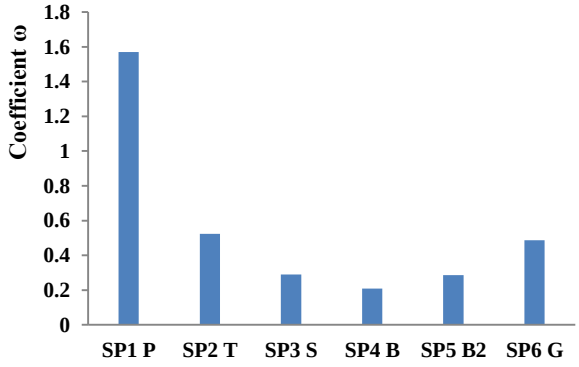

Figure 11: Coefficient ω

5.5 Validation with the analytic model

The bond-slip model, specifically applied to the interface between carbon fiber-reinforced polymer (CFRP) and concrete [23], is utilized in pull-out tests. These models are based on the concept of interface energy and involve the coefficient ω. Figures 12–17 clearly demonstrate that the bond-slip model arrived from the equation (1) accurately predicts the behavior of the interface. In case of brittle failure, such as SP1 P, SP2 T, and SP6 G, the analytical model also performs well. But for SP3 S and SP4 B, the analytical model underestimates the post peak behaviour, although the deviation is not significant. Consequently, the bond-slip model is recommended for predicting the bond-slip response with steel rods or bolts used in conjunction with a concrete interface. For the final constant stage, it can be a constant not zero for the not brittle cases SP3S, SP4B and SP5 B2.

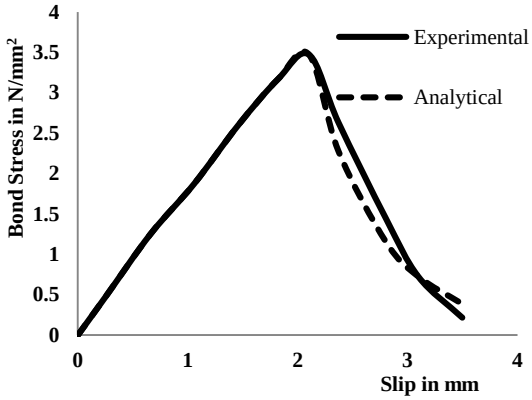

Figure 12: SP1 P (Plain rod)

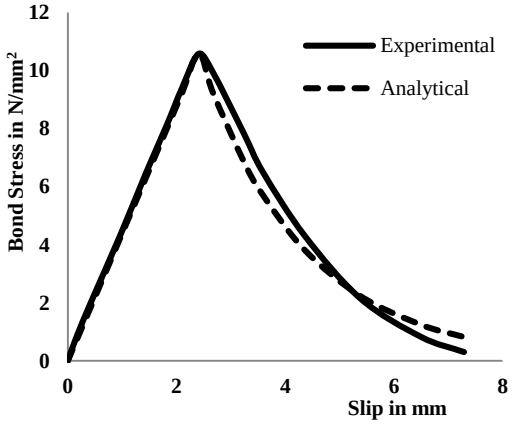

Figure 13: SP2 T (HYSD bar)

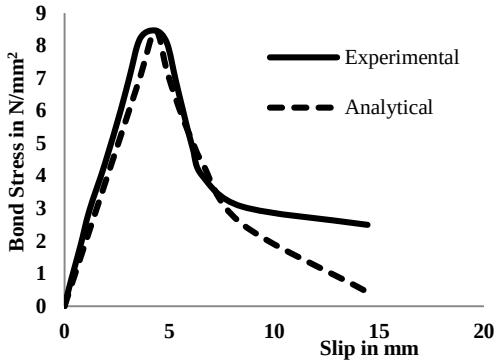

Figure 14: SP3 S (Fully threaded M12 bolt)

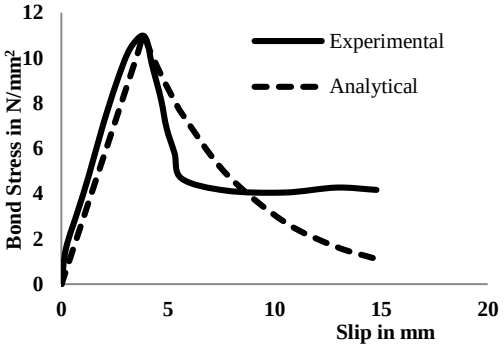

Figure 15: SP4 B (M12 bolt with washer nut)

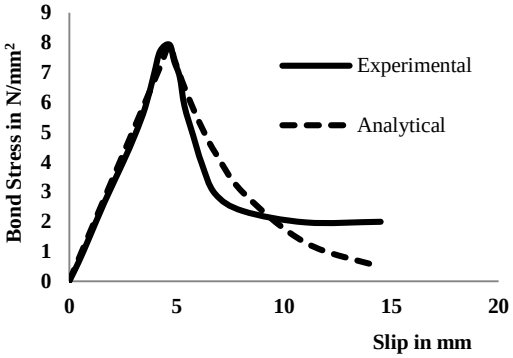

Figure 16: SP5 B2 (2 nos of M12 bolt with washer nut)

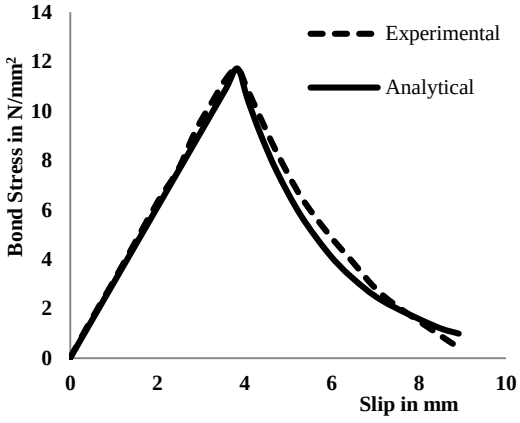

Figure 17: SP6 G (M12 bolt with washer nut in grout)

In summary, this study provides valuable insights on the behavior of plate embedment and offers a practical approach for achieving effective anchoring in construction applications. It also recommends the analytical approach to predict the bond – slip behaviour.

6 CONCLUSIONS

In conclusion, this research study focused on investigating the behavior of plate embedment and anchoring through rods and bolts. Pull-out tests were conducted to assess the bond-slip relationship, and a bond-slip model based on interface energy was utilized to validate the experimental findings. Based on the results, an effective embedment technique is proposed for the dry connections in precast system.

1. All specimens exhibited concrete cone break-out failure, except for SP1 P. In the case of plain rods, no bonding between the steel and concrete was observed, leading to slipping failure.
2. High-strength concrete improves the bond strength but results in brittle failure mode.
3. Despite having a shorter embedment length, SP4 B (bolt with washer nut arrangement) achieves a higher peak load and displays superior post-peak behavior due to the mechanical interlocking.
4. SP4 B performs well with a low coefficient ω and high interface fracture energy. Anchoring through bolts with washer nut arrangement is recommended for achieving effective embedment in precast panels.
5. The bond-slip model, used for CFRP and concrete interface, successfully applies to all specimens and validates well. This model can be recommended for predicting the bond-slip response of steel and concrete embedment as well.

REFERENCES

[1] Hemamalini, S., Vidjeapriya, R. and Jaya, K. P., 2021. Performance of precast shear wall connections under monotonic and cyclic loading: A State-of-the-Art Review 1307–1328, Sep.

[2] Singhal, S., Chourasia, A., Chellappa, S. and Parashar, J., 2019. Precast reinforced concrete shear walls: State of the art review. *Struct. Concr.* **20**: 886–898

[3] Kurama, Y. C., Sritharan, S., Fleischman, R. B., Restrepo, J. I., Henry, R. S., Cleland, N. M., Ghosh, S. K. and Bonelli, P., 2018. Seismic-resistant precast concrete structures: State of the Art. *J. Struct. Eng.* **144**: 03118001

[4] VanGeem, M., 2006. Achieving sustainability with precast concrete. *PCI J.* **51**: 42.

[5] Jaillon, L., Poon, C.-S. and Chiang, Y. H., 2009. Quantifying the waste reduction potential of using prefabrication in building construction in Hong Kong. *Waste Manag.* **29**: 309–320.

[6] Hofheins, C. L., Reaveley, L. D. and Pantelides, C. P., 2002. Behavior of welded plate connections in precast concrete panels under simulated seismic loads. *PCI J.* **47**: 122–133.

[7] Shen, S. D., Pan, P., Miao, Q. S., Li, W. F. and Gong, R. H., 2019. Behaviour of wall segments and floor slabs in precast reinforced concrete shear walls assembled using steel shear keys (SSKW). *Struct. Control Heal. Monit.* **26**: 1–15.

[8] Shen, S. D., Pan, P., Miao, Q. S., Li, W. F. and Gong, R. H., 2019. Test and analysis of reinforced concrete (RC) precast shear wall assembled using steel shear key (SSK). *Earthq. Eng. Struct. Dyn.* **48**: 1595–1612.

[9] Kalthoff, M. and Raupach, M., 2021. Pull-out behaviour of threaded anchors in fibre reinforced ordinary concrete and UHPC for machine tool constructions. *J. Build. Eng.* **33**: 101842.

[10] Tóth, M., Bokor, B. and Sharma, A. 2019. Anchorage in steel fiber reinforced concrete – concept, experimental

evidence and design recommendations for concrete cone and concrete edge breakout failure modes. *Eng. Struct.* **181**: 60–75.

[11] Wang, D., Wu, D., Ouyang, C. and Zhai, M.,2016 Performance and design of post-installed large diameter anchors in concrete, *Constr. Build. Mater.*, vol. 114, pp. 142–150.

[12] Zhao, C. A. O. Y., Gentian JIA Ran. and Gao Peng, Experimental study on pull-out performance of studs under monotonic and cyclic loading, *Journal of Building Structures*, vol. 40, no. 40S1. pp. 418–423.

[13] Li, F., Tang, H., Wen, T., Li, J., Chen, Z., Jiang, Y. and Gao, H., 2022. Pullout behavior of studs in ultra-high performance concrete with steel fibers and novel structural fibers. *Structures*. **44**: 405–417.

[14] Gil-Martín, L. M. and Hernández-Montes, E., 2019. Reinforcement anchored in tension by heads. Review of capacity formulation and applicability limits. *Eng. Struct.* **184**: 186–193.

[15] Rybinski, M., 2014. Komponentenmethode für Ankerplatten mit Kopfbolzen unter einachsiger Beanspruchung.

[16] Seghezzi, H. D., 1986. Einflüsse der Belastungsgeschichte und der Umgebung (Effects of load history and environment). *Manuskript der Vor. Befestigungstechnik an der ETH Zürich, Sommersemester*. 1–8.

[17] Ožbolt, J., Eligehausen, R. and H. W. Reinhardt, H. W., 1999. Size effect on the concrete cone pull-out load, *Int. J. Fract.*, vol. 95, no. 1–4, pp. 391–404.

[18] Eligehausen, R., Mallée, R. and Silva, J. F., 2006. Anchorage in concrete construction, John Wiley & Sons.

[19] Eligehausen, R. and Ožbolt, J., 1990. Size effect in anchorage behavior. *Fract. Behav. Des. Mater. Struct.*

[20] Biscaia, H. C., Chastre, C., Borba, I. S., Silva, C. and Cruz, D., 2016. Experimental Evaluation of Bonding between CFRP Laminates and Different Structural Materials. *J. Compos. Constr.* **20**:.

[21] Liu, S., Yuan, H. and Wu, J., 2019. Full-range mechanical behavior study of FRP-to-concrete interface for pull-pull bonded joints. *Compos. Part B Eng.* **164**: 333–344.

[22] Caggiano, A., Martinelli, E., Schicchi, D. S. and Etse, G., 2018. A modified Duvaut-Lions zero-thickness interface model for simulating the rate-dependent bond behavior of FRP-concrete joints. *Compos. Part B Eng.* **149**: 260–267.

[23] Yuan, C., Chen, W., Pham, T. M., Hao, H., Jian, C. and Shi, Y., 2019. Strain rate effect on interfacial bond behaviour between BFRP sheets and steel fibre reinforced concrete. *Compos. Part B Eng.* **174**: 107032.

[24] Biscaia, H. C., Chastre, C. and Silva, M. A. G. 2013. Linear and nonlinear analysis of bond-slip models for interfaces between FRP composites and concrete. *Compos. Part B Eng.* **45**: 1554–1568.

[25] Ferracuti, B., 2006. Strengthening of RC structures by FRP: Experimental analyses and numerical modelling. *Univ. Bol. Bol.*